

# Using iTRAQ-Based Quantitative Proteomics Analysis to Identify Differentially Expressed Proteins Related to Larval Development of *Portunus trituberculatus*

CHEN Xiayue<sup>1)</sup>, MU Changkao<sup>1), 2), \*</sup>, LI Ronghua<sup>1)</sup>, YE Yangfang<sup>1)</sup>, SONG Weiwei<sup>1)</sup>, SHI Ce<sup>1)</sup>, LIU Lei<sup>1)</sup>, WANG Huan<sup>1)</sup>, and WANG Chunlin<sup>1), \*</sup>

1) Collaborative Innovation Center for Zhejiang Marine High-Efficiency and Healthy Aquaculture, Ningbo University, Ningbo 315211, China

2) Key Laboratory of Applied Marine Biotechnology, Ministry of Education, Ningbo University, Ningbo 315211, China

(Received June 24, 2020; revised August 3, 2020; accepted December 29, 2020)

© Ocean University of China, Science Press and Springer-Verlag GmbH Germany 2021

**Abstract** The swimming crab *Portunus trituberculatus* is an economically important marine crustacean species. Here isobaric tags for relative and absolute quantitation (iTRAQ) analysis were used to identify proteins that are differentially expressed during larval development of *P. trituberculatus* to elucidate the underlying mechanisms. In comparison with the first zoea stage (Z1), 3980 proteins were identified from 32789 peptides, which were matched with 115497 spectrums. A total of 241 proteins were screened with significantly differential expressions in all development stages. These 241 proteins are involved in various biological processes, such as cytoskeleton organization, protein synthesis, energy production and substance metabolism, physiological activities, and transport. Cluster analyses of the 241 differentially expressed proteins led to the generation of four protein clusters based on the overall similarity in protein expression patterns. Exactly 54, 70, 36, and 45 proteins clustered in profiles 10 (0, 0, 0, -1, 0, 0), 15 (0, 1, 0, 1, 0, 1), 18 (0, 1, 2, 2, 1, 0), and 19 (0, 1, 2, 3, 4, 5), respectively. Muscle development and exoskeleton renewal were important processes throughout the development stages. In addition, protein synthesis, degradation, and digestion actively occurred, especially at the Z4 stage. These results provide novel insights into the mechanisms underlying larval development of swimming crab and can assist in larval rearing.

**Key words** *Portunus trituberculatus*; iTRAQ; proteomics; larval development

## 1 Introduction

*Portunus trituberculatus* (Crustacea: Decapoda: Portunidae) is an economically important marine crab that is widely distributed throughout the four marginal seas in China (Xu *et al.*, 2009). Considering its large size, delicious flavor, and high nutritional value, this species has been favored by consumers for a long time. Since the mid-1990s, the swimming crab has been promoted for breeding and culture purposes in China to meet market demands (Wang *et al.*, 2010a). Larval rearing is essential for breeding and artificial culture; however, the survival rate of larvae is unstable in artificial culture, which has been a major obstacle for swimming crab hatcheries and restricted the industrial development of *P. trituberculatus*. Rearing the larvae of swimming crab for mass production is usually completed from the first zoea stage (Z1) to the first crab stage (C). Understanding the development of swimming crab larvae will contribute to providing theoretical basis for lar-

val rearing.

Genes regulate organism growth and development and other major traits. Nevertheless, the correlation between mRNA and protein expression levels is poor (Larsson *et al.*, 2013). Considering the occurrence of pre-, co-, and post-translational modifications, not all transcripts are translated (Feder and Walser, 2005). Proteins are thus an essential element for crustacean larvae undergoing these complex processes. Proteomics refers to the large-scale study and characterization of proteins and involves the investigation of their composition, functions, and expression levels and understanding their interactions and connections usually *via* biochemical methods. It has become a cutting-edge technique that is widely used in life sciences (Pandey and Mann, 2000; Zhang *et al.*, 2013). The iTRAQ enables protein level assessment using an isotope for peptide labeling. Its capability to analyze multiple samples (4 or 8) simultaneously facilitates time-course studies and allows the analysis of a large number of samples against the same control concurrently, saving sample preparation and analysis time and improving the experimental design (Pierce *et al.*, 2008; Unwin *et al.*, 2010). Thus, iTRAQ is a robust

\* Corresponding authors. E-mail: muchangkao@nbu.edu.cn  
E-mail: wangchunlin@nbu.edu.cn

method to study the mechanisms underlying larval development of *P. trituberculatus*.

Thus far, several attempts have been made to explore the larval development of different organisms, such as *Gadus morhua* (Sveinsdóttir *et al.*, 2008), *Crassostrea gigas* (Huan *et al.*, 2012), *Apis mellifera* (Li *et al.*, 2007), and *Bombyx mori* (Zhang *et al.*, 2014), using various proteomics techniques. These studies illustrated the importance of proteomics in understanding the molecular mechanisms responsible for larval development. The existing literature on larvae of swimming crabs primarily focuses on physiology, biochemistry, and artificial cultivation. Several studies have been conducted to explore the effects of pH (Yasunobu *et al.*, 1997), oxygen (Morioka *et al.*, 1988), harmful substances in water (Ren *et al.*, 2017), temperature and photoperiod (Wang *et al.*, 2004), artificial rearing (Dan *et al.*, 2016), morphogenesis (Dan *et al.*, 2014), and bait (Dan *et al.*, 2016) on the larvae of swimming crab. However, nearly no research has focused on the proteomics of larval development.

In the present study, iTRAQ was used to identify differentially expressed proteins (DEPs) related to the development of the larvae of swimming crab *P. trituberculatus*, which is helpful to understand the molecular mechanisms behind the development.

## 2 Materials and Methods

### 2.1 Animals and Samples

Experiments were performed at Jing-Ye Nursery Farm, Ningbo, China. Several spawning crabs were cultured in a cement tank with a volume of 30 m<sup>3</sup>. Water salinity and temperature were maintained at 24 ± 1 and 27 °C ± 2 °C, respectively. The crabs were fed daily with fresh mussels and chilled fish, whose weight was 5%–8% of the total weight of crabs. One spawning crab that was expected to hatch within 2 days was transferred to a plastic basket with an aeration device in the cement tank. Feeding was stopped before hatching. The larvae used in this experiment were all hatched from the same healthy spawning crab. After hatching, the larvae were freely scattered into the entire tank. The larval rearing method was performed as previously described by Wu *et al.* (2014). Briefly, rotifers *Brachionus plicatilis* (30–40 individuals mL<sup>-1</sup>) and microalgae *Platymonas subcordiformis* ((5–10) × 10<sup>4</sup> cells mL<sup>-1</sup>) were used to feed the Z stage 1–2 (Z1–Z2) larvae every 2 h, whereas *Artemia nauplii* (2 to 3 individuals mL<sup>-1</sup>) was provided to the Z3 stage (Z3)–megalopa (M) larvae.

The larvae of *P. trituberculatus* from the Z1 to first juvenile C were sampled to study the changes in protein composition at various developmental stages. Samples were collected when 70%–80% of the population had molted to the desired stage. The collected samples were immediately rinsed with sterilized seawater, snap frozen in liquid nitrogen, and then stored at –80 °C. Three biological replicates for each larval stage (Z1–Z4, M, and C) were used for subsequent analyses, and each sample contained more than 200 mg larvae.

### 2.2 Protein Extraction and Quality Control

The larval samples were ground to powder in liquid nitrogen. Total protein was extracted using a lysis buffer (7 mol L<sup>-1</sup> urea, 2 mol L<sup>-1</sup> thiourea, 4% CHAPS, 40 mmol L<sup>-1</sup> Tris-HCl, and pH 8.5) containing 1 mmol L<sup>-1</sup> phenylmethylsulfonyl fluoride and 2 mmol L<sup>-1</sup> (final concentration) ethylenediaminetetraacetic acid. After 5 min, dithiothreitol (DTT) with final concentration of 10 mmol L<sup>-1</sup> was added. The suspension was sonicated at 200 W for 15 min and then centrifuged at 4 °C at 30000 g for 15 min. The supernatant obtained was mixed well with 5 × volume of chilled acetone containing 10% (v/v) TCA and incubated at –20 °C overnight. After centrifugation at 4 °C, 30000 g, the supernatant was discarded. The precipitate was washed with chilled acetone three times. The pellet was air-dried and dissolved in lysis buffer mentioned above. The obtained supernatant was added with 10 mmol L<sup>-1</sup> (final concentration) DTT and incubated at 56 °C for 1 h. Subsequently, after cooling to room temperature, the sample was mixed with 55 mmol L<sup>-1</sup> (final concentration) iodoacetamide and incubated for 45 min in a dark room for alkylation. The supernatant was mixed well with 5 × volume of chilled acetone for 2 h at –20 °C and centrifuged at 4 °C at 30000 g for 15 min. The precipitate was dissolved in lysis buffer and centrifuged at 4 °C at 30000 g for 15 min. The supernatant was transferred to a new tube and quantified. Total protein concentration was subsequently measured using the Bradford method (Bradford, 1976).

### 2.3 Protein Digestion, iTRAQ Labeling, and Strong Cation Exchange (SCX) Fractionation

Total protein (100 µg) was collected from each sample solution and digested using Trypsin Gold (Promega, USA) with the protein: trypsin ratio of 30: 1 at 37 °C for 16 h. Subsequently, the peptides were dried by vacuum centrifugation, reconstituted in 0.5 mol L<sup>-1</sup> triethylammonium bicarbonate, and then processed with 8-plex iTRAQ reagent in accordance with manufacturer's instructions (Applied Biosystems, USA). The proteins from Z1, Z2, Z3, Z4, M, and C larval samples were labeled with iTRAQ reagents 115, 116, 117, 118, 119, and 121, respectively. SCX chromatography was executed on an LC-20AB high-performance liquid chromatography (HPLC) pump system (Shimadzu, Japan). Each fraction was desalted using a StrataX desalination column and then lyophilized.

### 2.4 LC-Electrospray Ionization-Tandem Mass Spectrometry (MS/MS) Analysis Based on Triple TOF 5600

Each fraction was resuspended in buffer A (5% acetonitrile (ACN), 0.1% formic acid (FA)) and centrifuged at 20000 g for 10 min at 4 °C. The final peptide concentration was approximately 0.5 µg µL<sup>-1</sup> on average. Then, 5 µL supernatant was loaded on an LC-20AD nano HPLC system (Shimadzu, Kyoto, Japan) by the autosampler onto a 2 cm C18 trap column. Then, the peptides were eluted onto a 10 cm analytical C18 column (inner diameter: 75 µm) packed

in-house. The samples were loaded at  $8 \mu\text{L min}^{-1}$  for 4 min. A 35 min gradient was then run at  $300 \text{ nL min}^{-1}$  starting from 5% to 35% B (95% ACN, 0.1% FA), followed by a 5 min linear gradient to 80%, then a 2 min linear gradient to 80%, and finally returned to 5% in 1 min and maintained at this level for 10 min. Data acquisition was performed using Triple TOF 5600 (AB SCIEX, Concord, ON) fitted with a Nanospray III source (AB SCIEX, Concord, ON) and a pulled quartz tip as the emitter (New Objectives, Woburn, MA).

Data were acquired using an ion spray voltage of 2.5 kV, curtain gas of 30 psi, nebulizer gas of 15 psi, and an interface heater temperature of  $150^\circ\text{C}$ . MS was performed at a resolving power of  $\geq 30000$  full widths at half of the peak's maximum value for time of flight MS scans. For information-dependent acquisition, survey scans were acquired in 250 ms, and as many as 30 product ion scans were collected if exceeding a threshold of 120 counts per second and a 2+ to 5+ charge state were attained. The total cycle time was fixed to 3.3 s. Q2 was 100 Da when the transmission window was for 100%. By monitoring the 40 GHz multi-channel time-to-digital conversion detector with four-anode/channel detection, four-time bins were summed for each scan at a pulse frequency value of 11 kHz. The  $35 \text{ eV} \pm 5 \text{ eV}$  sweeping collision energy setting coupled with iTRAQ-adjusted rolling collision energy was used in all precursor ions for collision-induced dissociation. The dynamic exclusion was set to 1/2 of peak width (15 s), and the precursor was refreshed from the exclusion list.

## 2.5 Data Analysis

Raw data files acquired from Orbitrap were converted into MGF files using Proteome Discoverer 1.2 (Thermo, 5600 msconverter), and the MGF files were searched. Protein identification was performed by using Mascot search engine (Matrix Science, London, UK; version 2.3.02) against a database containing 33942 sequences (a transcriptome database sequencing from multiple tissues and individuals at different developmental stages of *Portunus trituberculatus*). For protein identification, a mass tolerance of  $\pm 0.05$  Da was permitted for intact peptide masses and  $\pm 0.1$  Da for fragmented ions, with allowance for one missed cleavage in the trypsin digests. Gln- $\rightarrow$ pyro-Glu (N-term Q), oxidation (M), and deamidation were potential variable modifica-

tions, whereas carbamidomethyl iTRAQ 8-plex (N-term), and iTRAQ 8-plex (K) were fixed modifications. The charge states of peptides were set to +2 and +3. Specifically, an automatic decoy database search was performed in Mascot by selecting the decoy checkbox in which a random sequence of the database was generated and tested for raw spectra and the real database. Only peptides with significance scores ( $\geq 20$ ) at the 99% confidence interval by a Mascot probability analysis greater than the 'identity' were counted as identified to reduce the probability of false peptide identification. Each confident protein identification involved at least one unique peptide. Protein quantitation required that a protein contains at least two unique peptides. The quantitative protein ratios were weighted and normalized by the median ratio in Mascot. The ratios with  $P < 0.05$  and fold changes  $> 1.2$  were regarded as significant. Functional annotations of proteins were conducted using the Blast2GO program against the non-redundant protein database (National Center for Biotechnology Information). The Kyoto Encyclopedia of Genes and Genomes (KEGG) (<http://www.genome.jp/kegg/>) and EuKaryotic Orthologous Groups (KOG) (<http://www.ncbi.nlm.nih.gov/KOG/>) databases were used to classify and group the identified proteins, respectively. Using fold change  $> 1.2$  and  $P < 0.05$  as the cut-off criteria, significantly enriched Gene Ontology (GO) terms and KEGG signaling pathways were identified.

## 2.6 Real-Time Polymerase Chain Reaction (RT-PCR)

Table 1 lists the fluorescent quantitative primers used for RT-PCR, which was performed to measure mRNA expression levels. Six DEPs included chitoooligosaccharidolytic beta-N-acetylglucosaminidase (P49010), hemocyanin B chain (P10787), 40S ribosomal protein S8 (O76756), acyl carrier protein (Q94519), 6-pyruvoyl tetrahydrobiopterin synthase (Q9R1Z7), and stress-activated protein kinase c-Jun N-terminal kinase (JNK) (P92208). RPL18 (Ren and Pan, 2014) was used as the internal control gene. Quantitative RT-PCR (qRT-PCR) was performed using GoTaq<sup>®</sup> qPCR Master Mix (Promega, USA) on an ABI 7500 Fast Real-time PCR System (Applied Biosystems, USA) following the manufacturer's instructions. The total reaction volume was  $20 \mu\text{L}$ , and the reaction mixture contained  $1.5 \mu\text{L}$  cDNA and  $0.5 \mu\text{L}$  (final concentration:  $10 \text{ mmol L}^{-1}$ ) of

Table 1 List of genes with their respective forward and reverse primers used for RT-PCR analysis

Accession <sup>†</sup>	Forward/Reverse primer sequence (5'→3')	Annealing temperature (°C)	Product length (bp)
Q9R1Z7	GACCCAAATCAGGAAGACA GTGAGCACAGCAGAAAACA	60	205
Q94519	CCGGATGATGTCAGCTGGT CTTGGCTTGGATTCCCTAG	60	117
O76756	GTGTGGTGGATGTGGTGTA CAAGAGGGAGGGCATAGTG	60	135
P49010	GCTCTTTCACCAATGCCTCCCTCA CGTACCACTTCTGCTCACA	60	165
P10787	GGCAACGCTGCTTTCTTCC ACGCGCTGCTCCTTATTCT	60	243
P92208	AGGGTAGCGAGGACGGTTT GTTGGGTGCATCATGGGAG	60	171

Note: <sup>†</sup> Protein accession numbers in UniProt.

each primer. The amplification procedure included an initial denaturation step at 95°C for 30s, followed by 40 cycles at 95°C for 5s and 60°C for 20s. Each sample was run in triplicate. The relative expression levels were calculated using the  $2^{-\Delta\Delta Ct}$  method (Livak and Schmittgen, 2001); Z1 larvae served as the control group. All data are expressed as means  $\pm$  standard error (SE). SPSS 22 (IBM) was used for statistical analysis. Values were considered statistically significant when  $P < 0.05$ .

### 3 Results

#### 3.1 Protein Profiling

Upon iTRAQ analyses of *P. trituberculatus*, 115497 spectrums, 32789 peptides, and 3980 proteins were obtained as

shown in Fig. 1A with a false discovery rate of 1%. Overall, the protein mass distribution showed that protein mass above 100kDa accounted for 7.46%, and the protein mass between 10 and 60kDa accounted for 73.42% of the total proteins, respectively. In addition, the protein mass between 20 and 30kDa was the most prevalent (shown in Fig. 1B). Known proteins from the six stages were used as references in the KOG database to analyze the functional distribution of the identified proteins. Functional classification results revealed that most of the proteins were involved in ‘signal transduction mechanisms’ followed by ‘post-translational modification, protein turnover, chaperones’ and ‘general function prediction’. ‘General function prediction’ indicated that the function of several proteins was unknown (Fig. 1C).

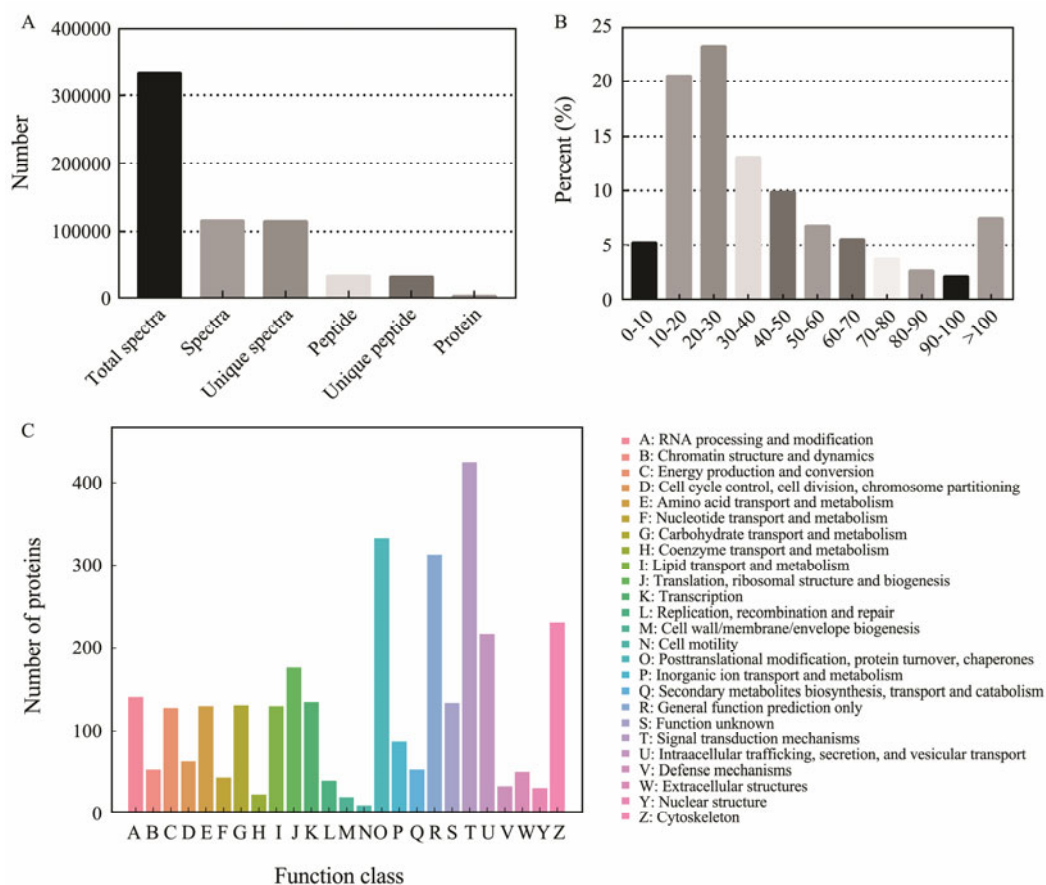


Fig. 1 Basic information and statistics for iTRAQ analysis of *Portunus trituberculatus* larval development proteome. (A), Coverage of proteins by the identified peptides; (B), distribution of identified proteins among various molecular weights (in kilodaltons); (C), clusters of orthologous groups for eukaryotic complete genome (KOG) annotation. All putative proteins were aligned to the KOG database and can be classified into at least 25 families.

#### 3.2 Quantitative Characteristics of DEPs

The highest amount of DEPs was found in Z4\_vs\_Z1 ( $n=1289$ ). In Z2\_vs\_Z1, C\_vs\_Z1, and M\_vs\_Z1, a smaller but considerable number of DEPs were observed ( $n=1288$ , 1158, 916, respectively). The least amount of DEPs was found in Z3\_vs\_Z1 ( $n=666$ ), but Z3\_vs\_Z1 showed the most massive amount of down-regulated proteins (Fig. 2A).

An upset diagram (Fig. 2B) was created to realize the overlap in DEPs between Z1 and the other five stages. In

total, 411 DEPs were found only in one stage, of which Z2 showed the largest number of DEPs ( $n=113$ ). Furthermore, Z4 stage had 111 DEPs, whereas Z3 showed the least number of DEPs ( $n=44$ ). Overall, 241 DEPs were detected during the whole developmental stages. Of these DEPs, 29 cytoskeleton organization proteins, 69 protein synthesis related proteins, 34 energy production and substance metabolism proteins, 9 physiological proteins, and 30 transport proteins were screened and part of them are listed in Table 2.

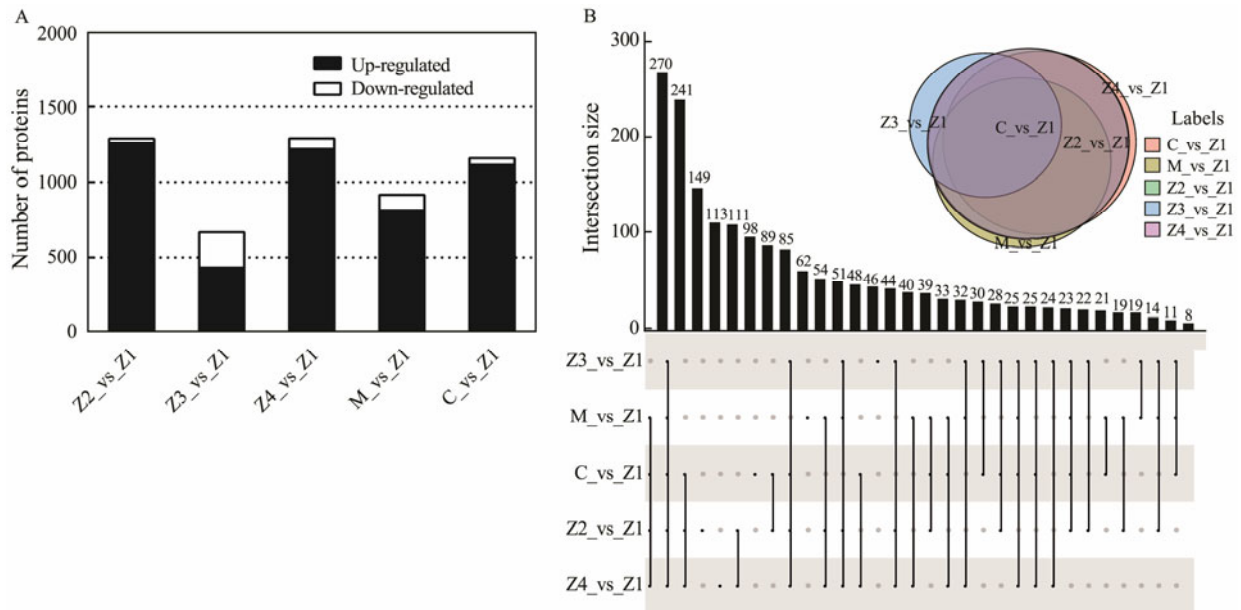


Fig.2 The DEPs were evaluated by iTRAQ analysis. (A), The number of up- or down-regulated (more than 1.2-fold) proteins in comparison with Z1; (B), the upset diagram of DEPs.

Table 2 List of DEPs at all the developmental stages

Protein	Accession <sup>†</sup>	Z2_vs_Z1 <sup>††</sup>	Z3_vs_Z1 <sup>††</sup>	Z4_vs_Z1 <sup>††</sup>	M_vs_Z1 <sup>††</sup>	C_vs_Z1 <sup>††</sup>
Actin, clone 302 (Fragment)	P18602	3.06	0.61	4.14	1.83	1.84
Actin, clone 403	P18603	3.54	0.83	2.21	2.21	2.93
Actin-2	P10984	5.67	1.30	2.04	4.01	14.25
Cuticle protein CP1158	P81580	2.75	1.56	6.07	6.60	2.20
Myosin heavy chain, muscle	P05661	2.21	1.40	3.53	3.24	3.35
Myosin heavy chain, non-muscle	Q99323	1.96	1.32	3.18	1.65	1.84
Myosin heavy chain, non-muscle	Q99323	2.31	1.64	3.34	2.25	2.04
Myosin-2 heavy chain	P08799	2.17	1.22	4.75	2.31	1.76
Myosin-2 heavy chain	P08799	1.50	1.31	1.53	1.92	1.88
Myosin-3	P12847	1.34	1.30	2.10	1.58	2.89
Myosin-9	Q62812	1.46	1.63	2.17	2.21	4.36
Myosin-9	P14105	1.90	2.85	3.75	2.03	2.43
Titin	A2ASS6	1.36	1.89	1.60	1.25	1.97
Titin	Q8WZ42	1.90	1.57	3.10	2.00	2.81
Titin	Q9I7U4	1.71	1.92	3.18	2.37	2.20
Titin	Q8WZ42	1.54	2.87	6.64	3.38	1.23
Titin	A2ASS6	1.52	1.88	2.22	2.14	3.47
Tubulin beta chain	P11833	2.20	0.74	1.62	1.57	2.27
Transcriptional regulator ATRX homolog	Q9U7E0	2.80	2.78	8.30	2.36	1.74
26S proteasome non-ATPase regulatory subunit 4	P55036	1.73	2.18	5.96	2.32	1.41
26S proteasome non-ATPase regulatory subunit 6	Q9V3G7	2.10	0.78	2.31	1.30	1.50
40S ribosomal protein S2	P49154	4.12	1.43	3.79	1.50	3.61
40S ribosomal protein S27	P55833	2.40	1.50	3.87	2.37	2.49
40S ribosomal protein S3	Q3T169	3.16	2.61	6.28	3.27	2.03
40S ribosomal protein S8	O76756	2.46	2.32	7.70	1.73	2.07
60S ribosomal protein L12	P35979	2.58	1.95	3.19	2.11	2.10
60S ribosomal protein L23	Q3T057	1.50	1.37	2.70	1.44	1.99
60S ribosomal protein L27	Q7ZV82	2.53	2.06	5.70	2.61	3.20
60S ribosomal protein L3	O16797	2.09	1.25	2.60	2.55	2.29
60S ribosomal protein L44	Q9NB33	1.79	1.57	2.11	1.98	1.59
60S ribosomal protein L6	Q6QMZ4	4.25	1.30	3.39	2.70	3.87
60S ribosomal protein L7	P32100	2.13	1.38	4.03	1.62	1.95
Eukaryotic initiation factor 4A-II	Q3SZ65	1.90	1.23	2.50	2.40	2.35
Eukaryotic translation initiation factor 3 subunit C	Q17Q06	2.53	1.63	2.27	1.60	1.43

(to be continued)

(continued)

	Protein	Accession <sup>†</sup>	Z2_vs_Z1 <sup>††</sup>	Z3_vs_Z1 <sup>††</sup>	Z4_vs_Z1 <sup>††</sup>	M_vs_Z1 <sup>††</sup>	C_vs_Z1 <sup>††</sup>
	Eukaryotic translation initiation factor 3 subunit E-A	Q6DRI1	2.19	1.52	2.39	1.73	1.62
	Eukaryotic translation initiation factor 3 subunit H	Q9GV27	1.54	1.27	4.03	1.52	1.64
	Eukaryotic translation initiation factor 5	P55010	3.24	1.37	3.01	1.99	2.93
	Eukaryotic translation initiation factor 5A	P62924	1.89	1.71	3.78	2.46	1.82
	Chitooligosaccharidolytic beta-N-acetylglucosaminidase	P49010	3.57	3.61	17.68	2.82	1.50
	ATP synthase subunit O, mitochondrial	Q24439	2.20	1.87	6.57	1.74	2.40
Energy production and substance metabolism	Phosphoglycerate mutase 2	Q32KV0	1.48	1.44	4.23	2.22	1.47
	Chymotrypsin BII	P36178	2.26	2.04	3.25	1.59	4.57
	Phosphoglycerate kinase	Q01604	3.80	1.30	3.15	2.56	4.88
	Glycogen phosphorylase	Q9XTL9	3.01	1.50	3.07	1.69	1.92
	Glucose-6-phosphate isomerase	P52031	1.92	1.37	2.91	1.34	1.66
	Pyruvate kinase	O62619	1.55	0.70	2.33	1.21	1.40
	Succinyl-CoA ligase [GDP-forming] subunit beta, mitochondrial	Q9Z218	2.00	0.79	1.61	1.75	1.29
	Pseudo-hemocyanin-2 (Fragment)	Q6KF81	1.98	1.95	12.14	7.62	1.61
	Pseudo-hemocyanin-2 (Fragment)	Q6KF81	1.79	1.69	11.68	6.61	1.48
Physiological protein	Hemocyanin C chain	P80096	2.51	1.45	2.5	1.66	2.93
	Hemocyanin	P80888	4.26	4.42	6.33	3.55	5.86
	Hemocyanin subunit 2	P84293	4.25	1.91	3.8	2.22	4.48
	Hemocyanin	P80888	4.34	1.83	3.14	2.38	3.99
	Hemocyanin B chain	P10787	2.47	1.73	7.27	1.97	2.32
		ADP-ribosylation factor 1	P61209	2.19	0.83	1.63	1.65
	ADP-ribosylation factor 4	Q3SZF2	1.97	0.82	1.80	1.54	1.71
Transport protein	Exportin-1	Q6P5F9	2.20	0.71	1.78	1.87	1.89
	GTP-binding nuclear protein Ran	Q9VZ23	2.78	1.32	2.80	2.21	2.46
	Importin-5	O00410	2.06	1.26	2.26	1.43	1.33
	Ras-related protein Rab-1A	Q05974	2.05	0.77	1.77	1.42	1.52

Notes: <sup>†</sup> Protein accession numbers in UniProt; <sup>††</sup> The iTRAQ ratios for Z2, Z3, Z4, M, C using Z1 as control.

### 3.3 Enrichment and Cluster Analyses of the 241 DEPs

GO enrichment analysis was carried out to investigate the function of DEPs during larval development, and the top 20 GO terms of *P*-value were presented in scatterplots (Fig.3A). In the category of biological processes, the DEPs were mainly involved in 'signal peptide processing' (GO: 0006465), 'sarcomere organization' (GO: 0045214), 'glycolytic process' (GO: 0006096), and 'somatic muscle development' (GO: 0007525). In terms of cellular component, the DEPs were primarily related to 'lipid particle' (GO: 0005811), 'Z disc' (GO: 0030018), 'signal peptidase complex' (GO: 0005787), and 'DNA-directed RNA polymerase' (GO: 0000428). Finally, under the 'molecular function' category, 'chloride ion binding' (GO: 0031404), and 'copper ion binding' (GO: 0005507) were significantly enriched.

The main metabolic pathways of 241 DEPs during larval development were investigated by KEGG pathway enrichment analysis. Eight significantly enriched pathways were identified (Fig.3B), and they included 'riboflavin metabolism', 'protein processing in endoplasmic reticulum', 'protein export', 'tyrosine metabolism', 'RNA polymerase', 'N-glycan biosynthesis', 'ribosome', and 'complement and coagulation cascades'.

Regulatory patterns usually reflect the inherent involvement of proteins in corresponding biochemical pathways and can thus serve as a potential clue to the functional role

of these proteins. Proteins that shared the same expression profiles were grouped into 20 clusters using the STEM software to better understand the expression patterns of proteins that exhibited significant changes during larval development. With Z1 as the control, the expression levels at all developmental stages were normalized by log<sub>2</sub>, and then cluster analysis was performed. Short time-series clustering analysis revealed four significant expression patterns (*P* < 0.01) involved in larval development (Fig.4). A total of 54, 70, 36, and 45 proteins clustered in profiles 10 (0, 0, 0, -1, 0, 0), 15 (0, 1, 0, 1, 0, 1), 18 (0, 1, 2, 2, 1, 0), and 19 (0, 1, 2, 3, 4, 5), respectively. The largest group, Profile 15, contained 70 proteins whose expression levels were relatively high in Z2, Z4, and C stage. Profile 10 included 54 proteins whose expression patterns showed no evident change from the Z1 to Z3 stage. A marked increase and a subsequent decline in expression levels were noted during the transition from Z3 to M stage, followed by a balance in expression levels. Profile 19 included 45 proteins whose expression levels continually rose during the whole larval development. Profile 18 contained 36 proteins whose expression levels increased and reached the maximum at Z3 stage, maintained the maximum in the Z4 stage, and then decreased afterward. In addition, heat maps (Fig.5) are used to present cluster analysis of some important differentially expressed proteins, to more intuitively understand the expression characteristics of proteins at various developmental stages.



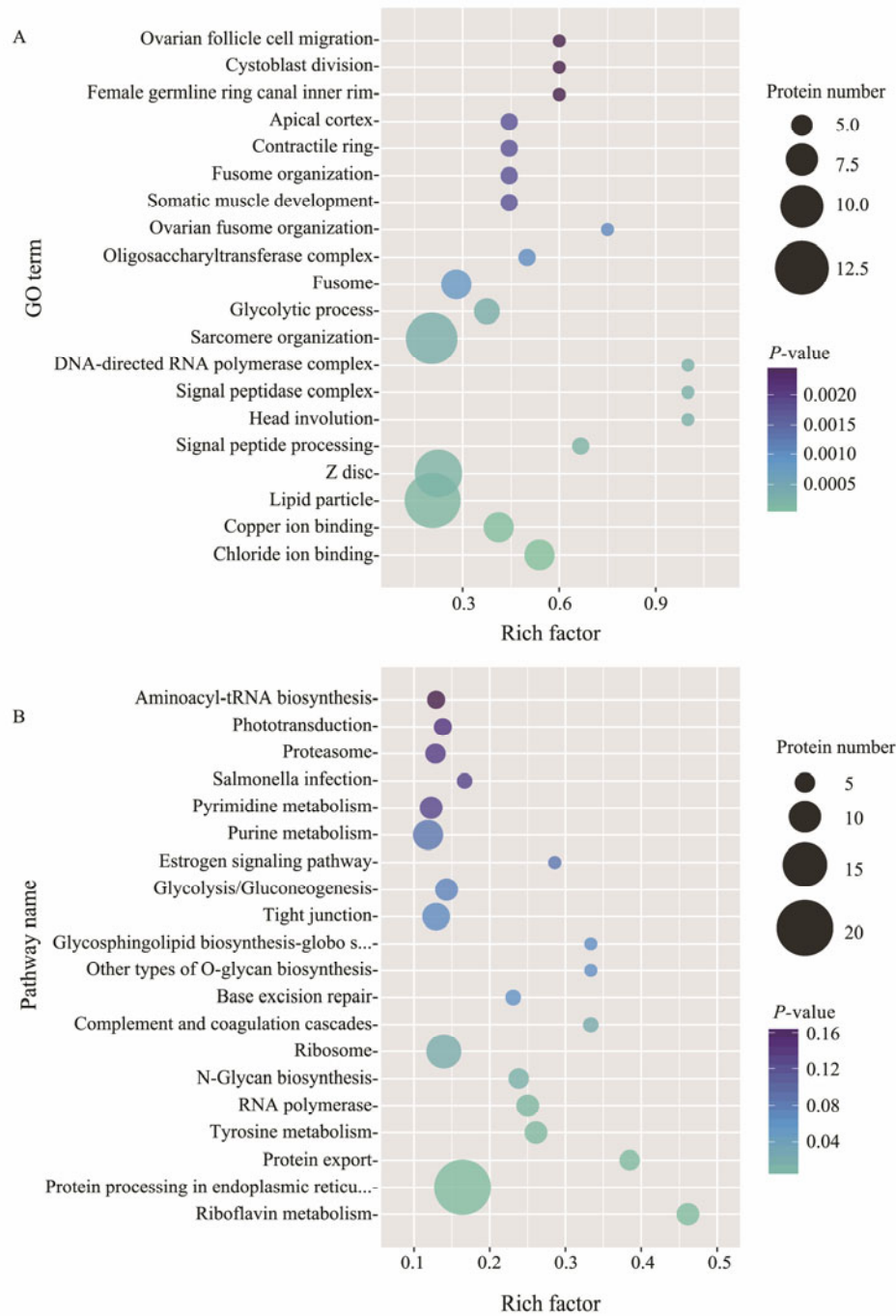


Fig.3 (A), GO enrichment analyses of 241 DEPs; (B), KEGG enrichment analyses of 241 DEPs. X-axis represents richness factors and Y-axis represents the functional classification of GO/KEGG.

### 3.4 Gene Expression Analysis by RT-PCR

qRT-PCR was used to elucidate the expression levels of genes encoding six DEPs to understand the correlation between proteins and their mRNA expression patterns (Fig.6). These genes expression patterns were roughly similar to those of their corresponding proteins, except that the expression levels of several proteins fluctuated at certain time points. For acyl carrier protein, except for stages Z3 and Z4, the expression trend in the protein was consistent with that in genes. With 40S ribosomal protein S8, except for stage Z4, the expression trend in the protein was consis-

tent with that in genes at different developmental stages. For stress-activated protein kinase JNK, except for the M stages, the expression trend in the protein was consistent with that in genes at other developmental stages. For chitinoglycosaminidase, the protein expression trend is consistent with the gene expression trend. For 6-pyruvoyl tetrahydrobiopterin synthase and hemocyanin, except for the M stages, the expression trend of the protein was consistent with that of genes in other developmental stages. The reasons for the inconsistency may be the time delay between the transcription and translation or the existence of post-translational modifica-

tion (Feder and Walser, 2005).

## 4 Discussion

In this study, iTRAQ was used to study the mechanisms underlying the larval development of *P. trituberculatus*. The combination of protein function enrichment and short time-series clustering analyses revealed key molecular characteristics and important stages in the development process, providing novel insights into pertinent mechanisms.

### 4.1 Cytoskeleton Organization

Larval development in crabs is accompanied by evident morphogenesis based on dynamic cytoskeleton reorganization. The cytoskeleton of eukaryotic cells consists of microtubules and microfilaments, which are composed of tubulin and actin, respectively. Actin and myosin also form sarcomere organization, which is a repeating unit of myofibrils in muscle cells (Rui *et al.*, 2010). Titin plays an important role in muscle contraction (Trinick and Tskhovrebova, 1999). Herein, tubulin, actin, titin, and myosin were

all detected and exhibited dynamic expression profiles during larval development of *P. trituberculatus*; the expression levels of most proteins were the highest at the Z4 or C stage (Fig. 6A). The GO terms ‘sarcomere organization’ and ‘somatic muscle development’ were enriched among 241 DEPs. These results indicate that muscle activity actively occurred during the development especially at Z4 and C stages. Similar expression level trends were reported in *Litopenaeus vannamei*, where the expression level of the gene encoding myosin significantly increased between the Z and mysis stages (Wei *et al.*, 2014). Furthermore, the expression level of myosin was used as a molecular marker for the growth potential of Atlantic pink shrimp (Kamimura *et al.*, 2008). Crustacean muscle growth is discontinuous and greatly affected by the molting cycle (Jung *et al.*, 2013); however, muscle protein synthesis is also essential for crustacean growth, reproduction, and other metabolic activities. Thus, many cytoskeletal proteins that were differentially expressed during larval development in *P. trituberculatus* confirmed the importance of muscle development.

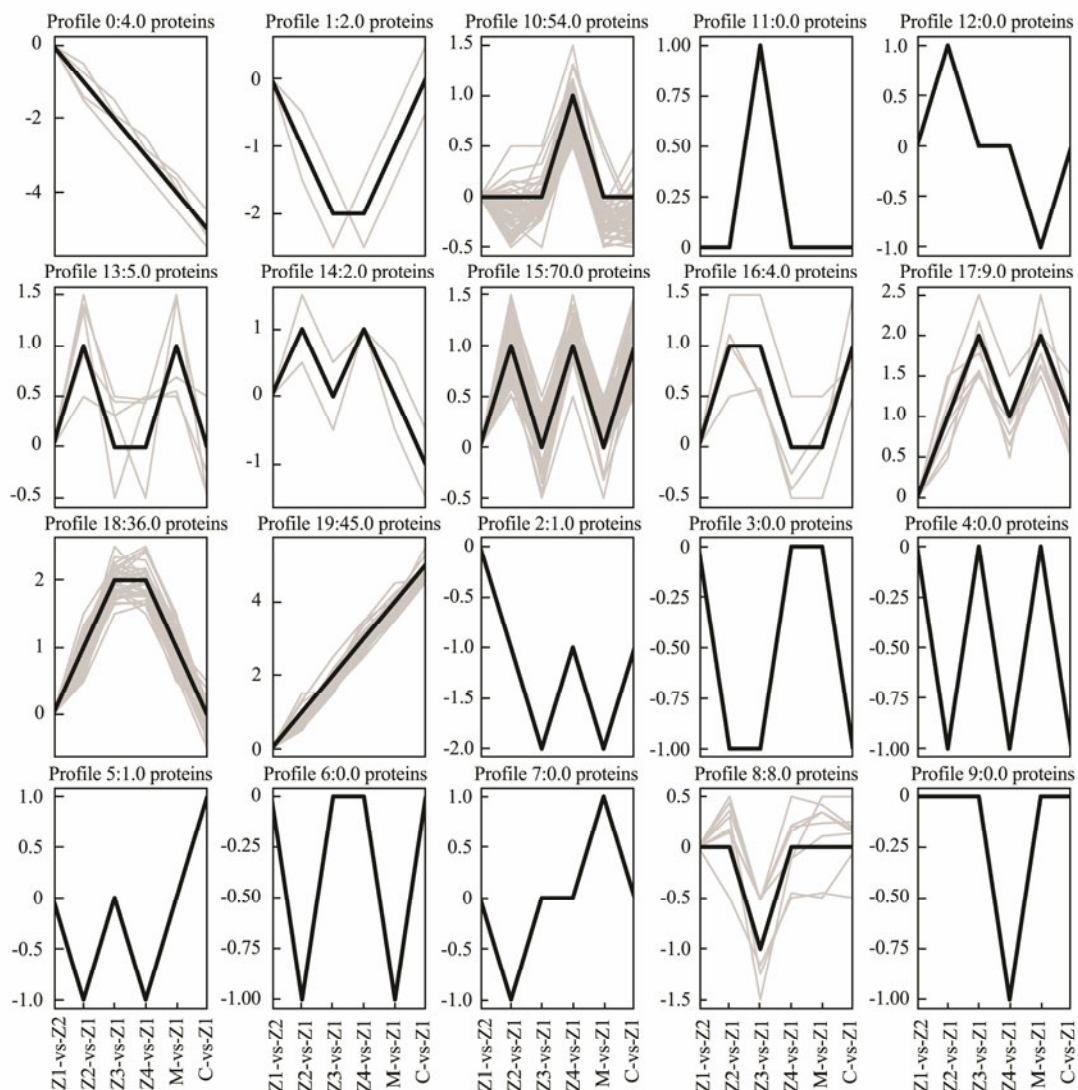


Fig. 4 Cluster analysis of DEPs during larval development. Profiles 10, 15, 18, and 19 were the four significant expression patterns ( $P < 0.01$ ) involved in larval development.



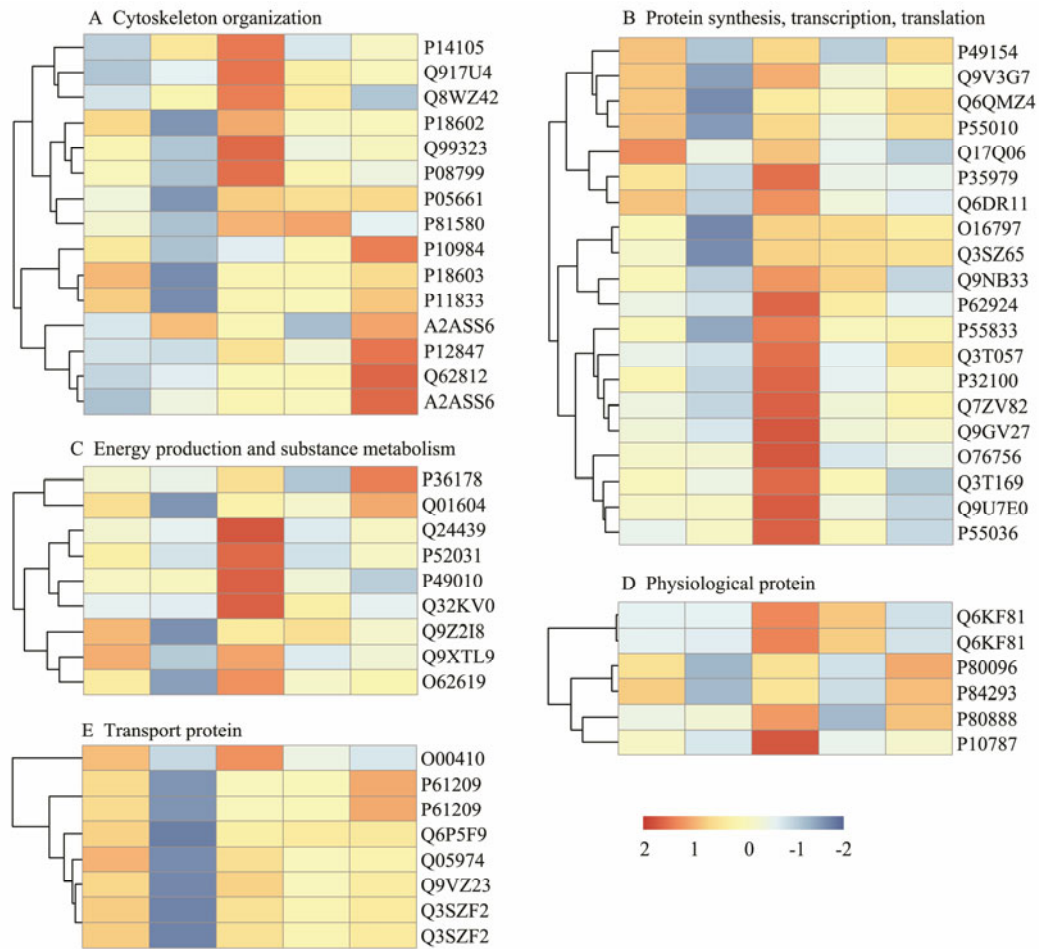


Fig.5 Cluster analyses. A heat map of the Z-score normalizing and log<sub>2</sub>-transformed relative abundance of proteins during Z1 concerning the remaining stages was created using iTRAQ-derived quantitative data. For each protein, an accession was provided. Grading represents the ratio of protein expression levels. The groups from left to right are Z2\_vs\_Z1, Z3\_vs\_Z1, Z4\_vs\_Z1, M\_vs\_Z1, and C\_vs\_Z1.

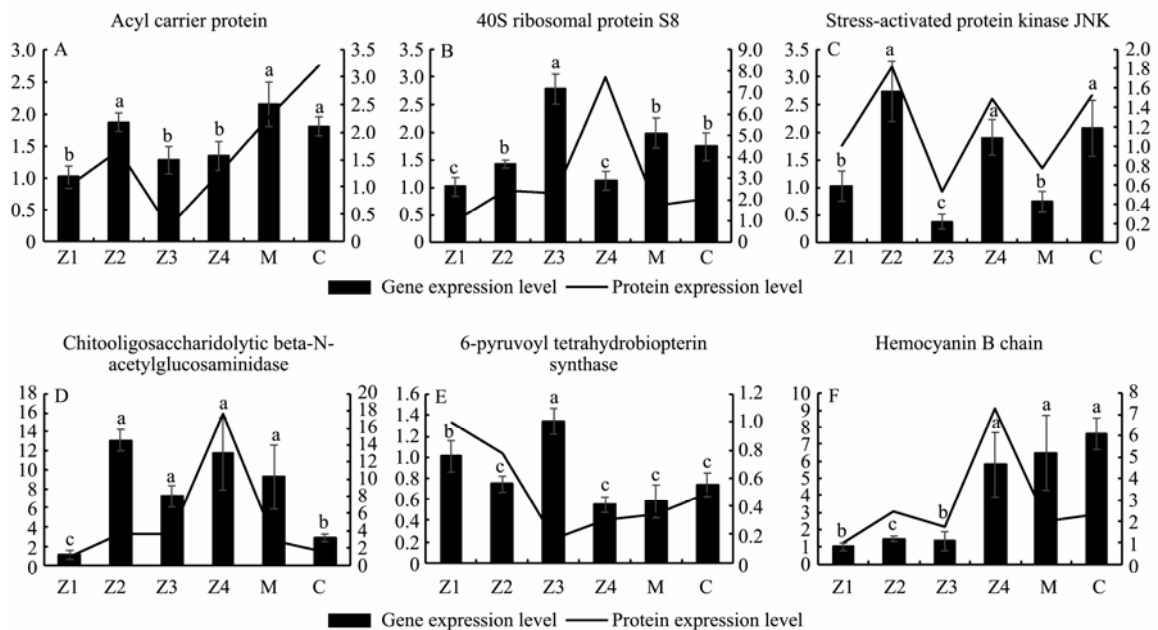


Fig.6 Comparison of expression values of six genes at protein and transcription levels at different stages by iTRAQ and real-time RT-PCR analysis. Histograms represent the relative expression levels as assessed by qRT-PCR and reported as means and SE of three biological replicates for each stage. Significantly different groups are indicated by different lower-case letters ( $P < 0.05$ ). Control: Z1 stage. The line graph represents the expression trend of protein ratio.

The crab epidermis is mainly composed of chitin, proteins, and calcium carbonate (Kuballa *et al.*, 2007). Cuticle proteins combine with chitin to form a fiber skeleton to control epidermal calcification, which played crucial role in the formation of the new epidermis. Cuticle protein genes reportedly have diverse expression patterns: they played distinct roles in different tissues (Karouzou *et al.*, 2007) or at different developmental stages (Soares *et al.*, 2011). In *Anopheles gambiae*, specific cuticle protein genes are expressed only at the pupal stage or before adult molting, indicating that they may be components of the pupal or adult epidermis. By contrast, other cuticle protein genes are highly expressed during the larval stage and may be involved in the formation of larval epidermis (Togawa *et al.*, 2008). In this study, cuticle protein (P81580) was differentially expressed in all developmental stages; its differential expression was relatively high in Z4 and M, with the peak appearing at M. This finding indicates that this protein may function differently at various stages. Other cuticle proteins were detected in each stage; Z4 showed two other differentially expressed cuticle proteins (P81576 and P81575). In insects, the physical properties of the epidermis and associated proteins extremely differ in various developmental stages and body parts (Charles, 2010). The morphology of M and juvenile crabs is different from that of other larvae, and individuals at Z4 and M need to be prepared for the morphological changes that will occur in the next stage. Therefore, we speculated the different epidermis compositions and the unique role of cuticle protein (P81580) at different developmental stages. Nevertheless, further studies are necessary to understand the specific role of this protein.

#### 4.2 Protein Synthesis, Transcription, and Translation

$\alpha$ -Thalassemia/mental retardation, X-linked (ATRX) is a member of the sucrose nonfermenting 2 family of helicase/ATPase, and it is believed to regulate gene expression via an effect on the chromatin structure and/or function (McDowell *et al.*, 1999). The gene encoding ATRX is required for embryonic development and somatic gonadal development of *Caenorhabditis elegans*. Moreover, the abrogation of a homolog of X-linked nuclear protein/ATRX in combination with the inactivation of genes of the nucleosome remodeling and deacetylase complex blocked larval development with a cessation of growth but not cell division (Cardoso *et al.*, 2005). Furthermore, the aberrant expression or activity of ATRX in humans and mice causes severe developmental abnormalities (Bérubé, 2011). Transcriptional regulator ATRX homolog (Q9U7E0) was up-regulated throughout development, with its expression level increasing by 8.8-fold at Z4 (Fig. 6B). This transcriptional regulator is necessary for larval development, but further studies are required to determine the cause for its sharply increased expression at Z4.

Protein synthesis is a complex yet conservative process and is essential for organism growth and development. Ribosomal proteins and rRNA compose ribosomes, which are large protein-RNA machines that use genetic information

to synthesize proteins in eukaryotic cells (Ramakrishnan, 2011). Ribosomal proteins are also related to the regulation of DNA replication, RNA processing, cell proliferation, and growth and development (Labriet *et al.*, 2019). Ribosomal protein S3 is indispensable for development, and its knockdown causes pre-implantation developmental arrest in mice (Peng *et al.*, 2019). During larval development, 11 ribosomal proteins were detected with different expression trends, and they were up-regulated in all stages, in which the 40S ribosomal protein S8 was up-regulated by 7.7-fold at Z4 (Fig. 6C). In addition, six eukaryotic initiation factors and an elongation factor were detected, and the expression levels of most of them were the highest in Z4. Initiation factors not only play an important role in translation but also participate in responding to other life activities. Eukaryotic translation initiation factor 5A-1 (eIF5A) is the only cellular protein that contains hypusine residues, which are necessary for its function; the eIF5A protein and deoxyhypusine/hypusine modification are essential for eukaryotic cell proliferation (Park, 2006). Elongation factors play a vital role in protein synthesis because they are involved in polypeptide chain extension (Andersen *et al.*, 2003). Two 26S proteasome non-ATPase regulatory subunits (P55036 and Q9V3G7) were identified, and their expression levels were the highest at Z4. The 26S proteasome plays a key role in maintaining protein homeostasis by eliminating misfolded or damaged proteins that may adversely affect cell function. Moreover, this proteasome removes proteins whose function is no longer needed (Schweitzer *et al.*, 2016). Therefore, during the complete development process, protein synthesis and degradation were active, especially in Z4, and this finding can be explained by the need of individuals in Z4 to prepare energy and materials for metamorphosis in the next stage. These protein synthesis-related proteins are necessary for the normal growth and development of larvae.

#### 4.3 Energy Production and Substance Metabolism

Chitin, a homopolymer of  $\beta$ 1-4-linked N-acetylglucosamine, is a key component of the crustacean exoskeleton. Chitooligosaccharidolytic beta-N-acetylglucosaminidase (P49010) is a crucial enzyme involved in chitin digestion in the chitinase system, and it plays a vital role in chitin degradation and synthesis (Nagamatsu *et al.*, 1995). In *Euphausia superba*, NAGase distributed in the epidermis is regulated by ecdysone, and it is massively synthesized to promote the degradation of chitin (Peters *et al.*, 1999). In crustaceans, periodic shedding of the exoskeleton is one of the most important physiological processes essential for growth and postembryonic development (Jung *et al.*, 2013). The expression level of chitooligosaccharidolytic beta-N-acetylglucosaminidase increased sharply by 4–5-fold during the transition from Z3 to Z4, and the level sharply decreased by 6–7-fold during the transition from Z4 to M (Fig. 6D). The expression profile, combined with the cuticle protein (P81580) expression profile, led us to hypothesize that at Z4, exoskeleton renewal is more active than that at other stages and that the epidermis is thoroughly

degraded. The epidermis composition may also differ.

With the growth and morphological changes of swimming crab larvae, the supply of energy and substance is essential to support the development. Several DEPs involved in glucose metabolism, tricarboxylic acid (TCA) cycle, and oxidative phosphorylation were detected; these DEPs included phosphoglycerate mutase 2, fructose-bisphosphate aldolase, phosphoglycerate kinase, glucose-6-phosphate isomerase, pyruvate kinase, and succinyl-CoA ligase subunit beta. Glycolysis and TCA cycle are essential for energy supply and metabolic intermediate formation in crabs (Hu, 1958; Kallapur *et al.*, 1983). Phosphoglycerate kinase catalyzes the reversible transfer of the 1-phosphoryl group from 1,3-bisphosphoglycerate to adenosine diphosphate (ADP), forming ATP and 3-phosphoglycerate, that is, the first ATP-generating step in the glycolytic pathway. When cells overproduce ATP, this reaction slows down. Subsequently, 3-phosphoglycerate is isomerized into 2-phosphoglycerate by phosphoglycerate mutase. In the final step of glycolysis, pyruvate kinase catalyzes substrate-level phosphorylation to form pyruvate and ATP molecules, similar to the step involving phosphoglycerate kinase. The expression level of phosphoglycerate kinase was relatively high in Z2, Z4, and C1. Further, the expression levels of phosphoglycerate mutase and pyruvate kinase were initially low. However, the expression levels sharply increased and peaked during Z4 and decreased during M and C1. These findings suggest that larvae at Z4 required more carbohydrates than those at M, which may be used to compensate for the energy consumed during metamorphosis from Z4 to M. Carbohydrates are more important for the early than for the late development of crustaceans (Johnston, 2003). Similar results (Li *et al.*, 2015) have also been reported for *E. sinensis*. Adenosine-triphosphate (ATP) synthase can directly generate ATP during oxidative phosphorylation, which is the main energy supply pathway in aerobic organisms (Chinopoulos and Adam-Vizi, 2009). In this study, the expression of ATP synthase subunit O (Q24439) was up-regulated by 6.57-fold in the Z4 stage and 1.74-fold in the M stage. These findings indicate the high energy demand of individuals at the Z4 stage.

Protein is also one of the key nutrients for animal growth and development. The expression trend of chymotrypsin BII (P36178) increased from Z4, reached the lowest at M, and recovered in the C. From the expression trend, in Z4, protein digestion was highly active, and more proteins may be digested at this stage. In a study exploring the effects of dietary protein content on the growth and protease activity of *E. sinensis*, the protein requirement at Z5 was greater than that at M (Pan *et al.*, 2005). Thus, there is a higher demand for protein at stage Z4 than at other stages. This result thus provides useful feeding-related information relevant to the larval rearing of *P. trituberculatus*.

#### 4.4 Physiological Proteins

Hemocyanin is a large copper-containing protein that transports oxygen in crustacean hemolymph. The hemocyanin superfamily comprises hemocyanins, pseudo-hemo-

cyanins, phenoloxidasases, hexamerins, and hexamerin receptors (Burmester, 2002). All hemocyanins were significantly up-regulated, showing different expression patterns (Fig. 6E). Hemocyanin provides oxygen for the respiratory metabolism of larvae. Additionally, oxygen consumption by *P. trituberculatus* larvae considerably varies at different developmental stages, with oxygen consumption increasing with the increase in body mass (Xu *et al.*, 2012). Considering the inconsistency in larval oxygen consumption and hemocyanin expression, we speculated that hemocyanin also plays other roles in larval development. Hemocyanin has phenoloxidase activity and antibacterial functions (Decker and Jaenicke, 2004), and five monomers of hemocyanin have weak phenol monooxygenase activity in the swimming crab (Fujieda *et al.*, 2019). Phenoloxidase is an important immune molecule and a vital component of the innate immune system in arthropods. Across the developmental stages, three stages were enriched with immune-related pathways, indicating that the immune response is active during these molting stages. Thus, given the up-regulation of hemocyanin, this protein might have an immune function.

Pseudo-hemocyanin is a non-respiratory protein that is structurally closely related to hemocyanins. Its levels vary in different individuals, and its synthesis is associated with the molting or reproductive cycle (Burmester, 1999). In this study, two fragments were identified as pseudo-hemocyanin with the same expression trend. The expression level was the highest at Z4, decreased at M, and returned to original levels at C. At present, although little research has been conducted on this protein, it has been detected in other proteomics studies involving the swimming crab (Fu *et al.*, 2018). The stage-specificity of pseudo-hemocyanin in the development of *P. trituberculatus* larvae needs further investigations.

#### 4.5 Transport Proteins

The biogenesis of ribosomes is a very complex and highly coordinated process, in which ribosomal proteins are first transferred into the nucleus, then assembled in the nucleolus with rRNA, and finally exported to the cytoplasm as ribosomal subunits. Active transport across the nuclear pore complex requires nuclear transport factors, namely, transport receptors, adaptor molecules, and constituents of the Ran GTPase system. Transport receptors can be classified into importins or exportins depending on their transport direction (Jäkel and Gürlich, 1998). Ran GTPase is a key regulator of nucleocytoplasmic transport during interphase (Han and Zhang, 2007). In this study, an exportin, importin, and the GTP-binding nuclear protein Ran showed different expression patterns (Fig. 6E). Furthermore, three other members of the Ras superfamily were differentially expressed: ADP-ribosylation factor 1, ADP-ribosylation factor 4, and Ras-related protein Rab-1A. ADP-ribosylation factors, which are highly conserved small GTP-binding proteins, are key regulators that control membrane trafficking and organelle structure (Duan *et al.*, 2016). The Rab subfamily has broad intracellular localization and

plays a pivotal role in vesicle formation, transport, adhesion, anchoring, and fusion (Stenmark and Olkkonen, 2001). Once again, these results collectively validate that protein renewal is very active during larval development in swimming crabs.

## 5 Conclusions

The quantitative changes of protein expression profile and the protein functional relationship during the larval development of *P. trituberculatus* were analyzed and discussed in our study. Functional analysis indicated that muscle growth is important in the development process. Protein synthesis, degradation, digestion, and transport actively occur throughout the development process. The epidermal composition may be different at various developmental stages. Z4 seems to be a relatively particular development stage, and the demand for energy and substances is relatively high at this stage. Thus, stage Z4 needs more attention in the larval rearing process compared with the other stages. Our data provide novel insights into larval development and improve our understanding of larval rearing in *P. trituberculatus*.

## Acknowledgements

We thank members of our laboratory for their stimulating discussion and helpful comments on this manuscript. This work was supported by the National Natural Science Foundation of China (No. 41676140), the Major Agriculture Program of Ningbo (No. 2017C110007), the Modern Technology System of Agricultural Industry (No. CARS-48), and the K C Wong Magana Fund in Ningbo University.

## References

- Andersen, G. R., Nissen, P., and Nyborg, J., 2003. Elongation factors in protein biosynthesis. *Trends in Biochemical Sciences*, **28** (8): 434-441.
- Bérubé, N. G., 2011. ATRX in chromatin assembly and genome architecture during development and disease. *Biochemistry and Cell Biology*, **89** (5): 435-444.
- Bradford, M. M., 1976. A rapid and sensitive method for the quantitation of microgram quantities of protein utilizing the principle of protein-dye binding. *Analytical Biochemistry*, **72** (1-2): 248-254.
- Burmester, T., 1999. Identification, molecular cloning, and phylogenetic analysis of a non-respiratory pseudo-hemocyanin of *Homarus americanus*. *Journal of Biological Chemistry*, **274** (19): 13217-13222.
- Burmester, T., 2002. Origin and evolution of arthropod hemocyanins and related proteins. *Journal of Comparative Physiology B*, **172** (2): 95-107.
- Cardoso, C., Couillault, C., Mignon-Ravix, C., Millet, A., Ewbank, J. J., Fontés, M., *et al.*, 2005. XNP-1/ATR-X acts with RB, HP1 and the NuRD complex during larval development in *C. elegans*. *Developmental Biology*, **278** (1): 49-59.
- Charles, J. P., 2010. The regulation of expression of insect cuticle protein genes. *Insect Biochemistry Molecular Biology*, **40** (3): 205-213.
- Chinopoulos, C., and Adam-Vizi, V., 2009. Mitochondria as ATP consumers in cellular pathology. *Biochimica et Biophysica Acta*, **1802** (1): 221-227.
- Dan, S., Ashidate, M., and Hamasaki, K., 2016. Improved method for culturing the swimming crab *Portunus trituberculatus* larvae to prevent mass mortality during seed production. *Fisheries Science*, **82** (1): 113-126.
- Dan, S., Kaneko, T., Takeshima, S., Ashidate, M., and Hamasaki, K., 2014. Eyestalk ablation affects larval morphogenesis in the swimming crab *Portunus trituberculatus* during metamorphosis into megalopae. *Sexuality and Early Development in Aquatic Organisms*, **1** (1): 57-73.
- Dan, S., Oshiro, M., Ashidate, M., and Hamasaki, K., 2016. Starvation of Artemia in larval rearing water affects post-larval survival and morphology of the swimming crab, *Portunus trituberculatus* (Brachyura, Portunidae). *Aquaculture*, **452**: 407-415.
- Decker, H., and Jaenicke, E., 2004. Recent findings on phenoloxidase activity and antimicrobial activity of hemocyanins. *Developmental and Comparative Immunology*, **28**: 673-687.
- Duan, Y., Li, J., Zhang, Z., Li, J., and Liu, P., 2016. Characterization of ADP ribosylation factor 1 gene from *Exopalaemon carinicauda* and its immune response to pathogens challenge and ammonia-N stress. *Fish & Shellfish Immunology*, **55**: 123-130.
- Feder, M. E., and Walser, J. C., 2005. The biological limitations of transcriptomics in elucidating stress and stress responses. *Journal of Evolutionary Biology*, **18** (4): 901-910.
- Fu, Y., Zhu, F., Liu, L., Lu, S., Ren, Z., Mu, C., *et al.*, 2018. iTRAQ-based proteomic analysis identifies proteins involved in limb regeneration of swimming crab *Portunus trituberculatus*. *Comparative Biochemistry and Physiology Part D*, **26**: 10-19.
- Fujieda, N., Yakiyama, A., and Itoh, S., 2019. Five monomeric hemocyanin subunits from *Portunus trituberculatus*: Purification, spectroscopic characterization, and quantitative evaluation of phenol monooxygenase activity. *Biochimica et Biophysica Acta*, **1804** (11): 2128-2135.
- Han, F., and Zhang, X., 2007. Characterization of a ras-related nuclear protein (Ran protein) up-regulated in shrimp antiviral immunity. *Fish & Shellfish Immunology*, **23**: 937-944.
- Hu, A. S., 1958. Glucose metabolism in the crab, *Hemigrapsus nudus*. *Archives of Biochemistry and Biophysics*, **5** (2): 387-395.
- Huan, P., Wang, H., Dong, B., and Liu, B., 2012. Identification of differentially expressed proteins involved in the early larval development of the Pacific oyster *Crassostrea gigas*. *Journal of Proteomics*, **75** (13): 3855-3865.
- Jäkel, S., and Görlich, D., 1998. Importin beta, transportin, RanBP5 and RanBP7 mediate nuclear import of ribosomal proteins in mammalian cells. *The EMBO Journal*, **17** (15): 4491-4502.
- Johnston, D. J., 2003. Ontogenetic changes in digestive enzyme activity of the spiny lobster, *Jasus edwardsii* (Decapoda; Palinuridae). *Marine Biology*, **143** (6): 1071-1082.
- Jung, H., Lyons, R. E., Hurwood, D. A., and Mather, P. B., 2013. Genes and growth performance in crustacean species: A review of relevant genomic studies in crustaceans and other taxa. *Reviews in Aquaculture*, **5** (2): 77-110.
- Kallapur, V. L., Ramamohanrao, Y., and Narasubhai, A. V., 1983. Glycolytic enzymes in the premolt field crab *Paratelphusa hydrodromus* (Milne-Edwards) (Crustacea). *Archives Internationales de Physiologie et de Biochimie*, **91** (2): 127-132.
- Kamimura, M. T., Meier, K. M., Cavalli, R. O., Laurino, J., Maggioni, R., and Marins, L. F., 2008. Characterization of growth-related genes in the south-western Atlantic pink shrimp *Farfantepenaeus paulensis* (Pérez-Farfante 1967) through a mo-

- dified DDRT-PCR protocol. *Aquaculture Research*, **39** (2): 200-204.
- Karouzou, M. V., Spyropoulos, Y., Iconomidou, V. A., Cornman, R. S., Hamdrakas, S. J., and Willis, J. H., 2007. Drosophila cuticular proteins with the R&R consensus: Annotation and classification with a new tool for discriminating RR-1 and RR-2 sequences. *Insect Biochemistry and Molecular Biology*, **37** (8): 754-760.
- Kuballa, A. V., Merritt, D. J., and Elizur, A., 2007. Gene expression profiling of cuticular proteins across the moult cycle of the crab *Portunus pelagicus*. *BMC Biology*, **5** (1): 45.
- Labriet, A., Lévesque, É., Cecchin, E., De Mattia, E., Villeneuve, L., Rouleau, M., *et al.*, 2019. Germline variability and tumor expression level of ribosomal protein gene RPL28 are associated with survival of metastatic colorectal cancer patients. *Scientific Reports*, **9** (1): 13008.
- Larsson, O., Tian, B., and Sonenberg, N., 2013. Toward a genome-wide landscape of translational control. *Cold Spring Harbor Perspectives in Biology*, **5** (1): a012302.
- Li, J., Li, H., Zhang, Z., and Pan, Y., 2007. Identification of the proteome complement of high royal jelly producing bees (*Apis mellifera*) during worker larval development. *Apidologie*, **38** (6): 545-557.
- Li, Y., Hui, M., Cui, Z., Liu, Y., Song, C., and Shi, G., 2015. Comparative transcriptomic analysis provides insights into the molecular basis of the metamorphosis and nutrition metabolism change from zoeae to megalopae in *Eriocheir sinensis*. *Comparative Biochemistry and Physiology Part D*, **13**: 1-9.
- Livak, K. J., and Schmittgen, T. D., 2001. Analysis of relative gene expression data using real-time quantitative PCR and the  $2^{-\Delta\Delta CT}$  method. *Methods*, **25** (4): 402-408.
- McDowell, T. L., Gibbons, R. J., Sutherland, H., O'Rourke, D. M., Bickmore, W. A., Pombo, A., *et al.*, 1999. Localization of a putative transcriptional regulator (ATRX) at pericentromeric heterochromatin and the short arms of acrocentric chromosomes. *Proceedings of the National Academy of Sciences*, **96** (24): 13983-13988.
- Morioka, Y., Kitajima, C., and Hayashida, G., 1988. Oxygen consumption, growth and calculated food requirement of the swimming crab *Portunus Trituberculatus* in its early developmental stage. *Nippon Suisan Gakkaishi*, **54** (7): 1137-1141.
- Nagamatsu, Y., Yanagisawa, I., Kimoto, M., Okamoto, E., and Koga, D., 1995. Purification of a chitoooligosaccharidolytic  $\beta$ -N-acetylglucosaminidase from *Bombyx mori* larvae during metamorphosis and the nucleotide sequence of its cDNA. *Bio-science, Biotechnology, and Biochemistry*, **59** (2): 219-225.
- Pan, L. Q., Xiao, G. Q., Zhang, H. X., and Luan, Z. H., 2005. Effects of different dietary protein content on growth and protease activity *Eriocheir sinensis* larvae. *Aquaculture*, **246** (1-4): 313-319.
- Pandey, A., and Mann, M., 2000. Proteomics to study genes and genomes. *Nature*, **405** (6788): 837-846.
- Park, M. H., 2006. The post-translational synthesis of a polyamine-derived amino acid, hyposine, in the eukaryotic translation initiation factor 5A (eIF5A). *Journal of Biochemistry*, **139**: 161-169.
- Peng, H., Zhao, Y., Chen, J., Huo, J., Zhang, Y., and Xiao, T., 2019. Knockdown of ribosomal protein S3 causes preimplantation developmental arrest in mice. *Theriogenology*, **129**: 77-81.
- Peters, G., Saborowski, R., Buchholz, F., and Mentlein, R., 1999. Two distinct forms of the chitin-degrading enzyme N-acetyl- $\beta$ -d-glucosaminidase in the Antarctic krill: Specialists in digestion and moult. *Marine Biology*, **134** (4): 697-703.
- Pierce, A., Unwin, R. D., Evans, C. A., Griffiths, S., Carney, L., Zhang, L., *et al.*, 2008. Eight-channel iTRAQ enables comparison of the activity of six leukemogenic tyrosine kinases. *Molecular & Cellular Proteomics*, **7** (5): 853-863.
- Ramakrishnan, V., 2011. The eukaryotic ribosome. *Science*, **331** (6018): 681-682.
- Ren, Q., and Pan, L., 2014. Digital gene expression analysis in the gills of the swimming crab (*Portunus trituberculatus*) exposed to elevated ambient ammonia-N. *Aquaculture*, **434**: 108-114.
- Ren, X., Wang, Z., Gao, B., Liu, P., and Li, J., 2017. Toxic responses of swimming crab (*Portunus trituberculatus*) larvae exposed to environmentally realistic concentrations of oxytetracycline. *Chemosphere*, **173**: 563-571.
- Rui, Y., Bai, J., and Perrimon, N., 2010. Sarcomere formation occurs by the assembly of multiple latent protein complexes. *PLoS Genet*, **6** (11): e1001208.
- Schweitzer, A., Aufderheide, A., Rudack, T., Beck, F., Pfeifer, G., Plitzko, J. M., *et al.*, 2016. Structure of the human 26S proteasome at a resolution of 3.9 Å. *Proceedings of the National Academy of Sciences*, **113** (28): 7816-7821.
- Soares, M. P., Silva-Torres, F. A., Elias-Neto, M., Nunes, F. M., Simoes, Z. L., and Bitondi, M. M., 2011. Ecdysteroid-dependent expression of the tweedle and peroxidase genes during adult cuticle formation in the honey bee, *Apis mellifera*. *PLoS One*, **6** (5): e20513.
- Sveinsdóttir, H., Vilhelmsson, O., and Gudmundsdóttir, Á., 2008. Proteome analysis of abundant proteins in two age groups of early Atlantic cod (*Gadus morhua*) larvae. *Comparative Biochemistry and Physiology Part D*, **3**: 243-250.
- Stenmark, H., and Olkkonen, V. M., 2001. The Rab GTPase family. *Genome Biology*, **2** (5): REVIEWS3007.
- Togawa, T., Dunn, W. A., Emmons, A. C., Nagao, J., and Willis, J. H., 2008. Developmental expression patterns of cuticular protein genes with the R&R Consensus from *Anopheles gambiae*. *Insect Biochemistry and Molecular Biology*, **38** (5): 508-519.
- Trinick, J., and Tskhovrebova, L., 1999. Titin: A molecular control freak. *Trends in Biochemical Sciences*, **9** (10): 377-380.
- Unwin, R. D., Griffiths, J. R., and Whetton, A. D., 2010. Simultaneous analysis of relative protein expression levels across multiple samples using iTRAQ isobaric tags with 2D nano LC-MS/MS. *Nature Protocols*, **5** (9): 1574-1582.
- Wang, C., Jiang, L., Wang, R., and Li, Y., 2010. Effect of abrupt and gradual changes in salinity on development and feeding in juvenile swimming crab (*Portunus trituberculatus*). *Fisheries Science*, **29** (9): 510-514 (in Chinese with English abstract).
- Wang, J., Li, J., Kang, K., and Cheng, Y., 2004. Effects of water temperature and photoperiod on survival, and metamorphosis of *Portunus trituberculatus* larvae. *Journal of Beijing Fisheries*, **1**: 8-10 (in Chinese with English abstract).
- Wei, J., Zhang, X., Yu, Y., Huang, H., Li, F., and Xiang, J., 2014. Comparative transcriptomic characterization of the early development in Pacific white shrimp *Litopenaeus vannamei*. *PLoS One*, **9**: e106201.
- Wu, X., Zeng, C., C., and Southgate, P., 2014. Ontogenetic patterns of growth and lipid composition changes of blue swimmer crab larvae: Insights into larval biology and lipid nutrition. *Marine and Freshwater Research*, **65** (3): 228-243.
- Xu, J., Wang, C., Mu, C., and Zhang, L., 2012. Relationship between oxygen consumption and oxygen consumption rate and the body mass of *Portunus trituberculatus* at its early development stages. *Journal of Marine Science*, **30** (1): 102-106



- (in Chinese with English abstract).
- Xu, Q., Liu, R., and Liu, Y., 2009. Genetic population structure of the swimming crab, *Portunus trituberculatus* in the East China Sea based on mtDNA 16S rRNA sequences. *Journal of Experimental Marine Biology and Ecology*, **371** (2): 121-129.
- Yasunobu, H., Nagayama, H., Nakamura, K., and Hatai, K., 1997. Prevention of a fungal infection in the swimming crab *Portunus trituberculatus* larvae by high pH of rearing water. *Nippon Suisan Gakkaishi*, **63** (1): 56-63.
- Zhang, Y., Fonslow, B. R., Shan, B., Baek, M. C., and Yates 3rd, J. R., 2013. Protein analysis by shotgun/bottom-up proteomics. *Chemical Review*, **113**: 2343-2394.
- Zhang, Y., Dong, Z., Wang, D., Wu, Y., Song, Q., Gu, P., *et al.*, 2014. Proteomics of larval hemolymph in *Bombyx mori* reveals various nutrient-storage and immunity-related proteins. *Amino Acids*, **46** (4): 1021-1031.

(Edited by Qiu Yantao)